

## A MAMMOSITE MULTILUMEN (MS-ML) BALLOON USED FOR ACCELERATED PARTIAL BREAST IRRADIATION

A.R. STAN<sup>1</sup>, M. ALECU<sup>1</sup>, R. ALECU<sup>2</sup>, S. BOTH<sup>3</sup> and O. COZAR<sup>4,5</sup>

<sup>1</sup> Department of Medical Physics, AROS, Colleyville, TX

<sup>2</sup> Education Health and Research International, Colleyville, TX

<sup>3</sup> University of Pennsylvania, Medical Physics Division, Department of Radiation Oncology, Philadelphia, PA

<sup>4</sup> Babes-Bolyai University, Department of Physics, Cluj-Napoca, Romania,

<sup>5</sup> Academy of Romanian Scientists, 54 Splaiul Independentei, RO-050094. Bucharest, Romania

E-mail: onuc.cozar@phys.ubbcluj.ro

*Received April 2, 2012*

The optimum design for *MammoSite Multilumen* (MSML) device used in *Accelerated Partial Breast Irradiation* (APBI) has been studied. A number of ten test devices were used with a saline solution containing 5 vol.% contrast liquid suspended in a water phantom which was *Computer Tomograph* (CT) scanned. Various balloon to skin distances were considered. The following parameters were evaluated using dose volume histograms (DVHs): *Coverage Index* (CI), *Max Dose to Skin* (MSD) and *External Index* (EI). All these proved to be a better dosimetric choice than the classic MammoSite.

*Key words:* APBI, MammoSite multilumen, dosimetry, DVHs.

### 1. INTRODUCTION

*Accelerated Partial Breast Irradiation* (APBI) has become in the last decade a popular choice in *Breast Conserving Therapy* (BCT). Several studies have shown that the outcome of BCT in terms of local control and survival rates is comparable with that of modified radical mastectomy for early stage breast cancers [1–4].

In its early days, the APBI was carried out as interstitial brachytherapy, a method that was not largely embraced by many centers mainly due to the complexity of this procedure [5–8]. In addition, highly conformal external beam and intraoperative radiotherapy with photons and electrons were employed as APBI treatment techniques [9–12]. Then the MammoSite (MS) a number of studies concerning the dosimetric characteristics, reliability, safety as well as weaknesses of the MS device were reported [13–20].

In recent years the multicatheter device concept was developed, tested and introduced in clinical practice. *Strut Adjusted Volume Implant* (SAVI, Cianna Medical, Aliso Viejo, CA) and *Contura Multilumen-Balloon* (Contura MLB, SenoRx, Inc., Irvine, CA) are probably the most popular multicatheter devices to date. A number of papers compared the single-lumen MS device with newly designed multicatheter configurations and showed that the latter provides a greater flexibility in planning and also improvement in terms of minimizing the dose to the normal tissue [21–28].

The present study was conducted to obtain dosimetry data used to determine the best design for a new multilumen MammoSite device (MSML). All test devices are balloon-based multilumen brachytherapy applicators intended to be used for APBI. These were evaluated against the predicate device dosimetric attributes and for their potential to enhance dosimetric flexibility. The relative dosimetric strengths and weaknesses of the different MSML design prototypes were compared for different clinical situations, dose optimization and coverage constraints.

## 2. MATERIALS AND METHODS

### 2.1. DEVICE DESCRIPTION AND SELECTION

Ten prototype balloons were evaluated for dosimetric characteristics. All test devices are 4–5 cm variable diameters spherical, multilumen polyurethane balloons with 3 mm lumen center to balloon shaft center spacing (test devices 1–5), and 2 mm lumen center to balloon shaft center spacing configurations (test devices 6–10). All tested balloons configurations are presented in Table 1 and eight of the cross-sections in Figure 1.

*Table 1*

Description of test devices

Test Device #	Balloon configuration
1, 6	4 lumen, w/ central lumen
2, 7	3 lumen, no central lumen
3, 8	3 lumen, w/ central lumen, lumens in same plane
4, 9	2 lumen, w/ central lumen
5, 10	2 lumen, no central lumen

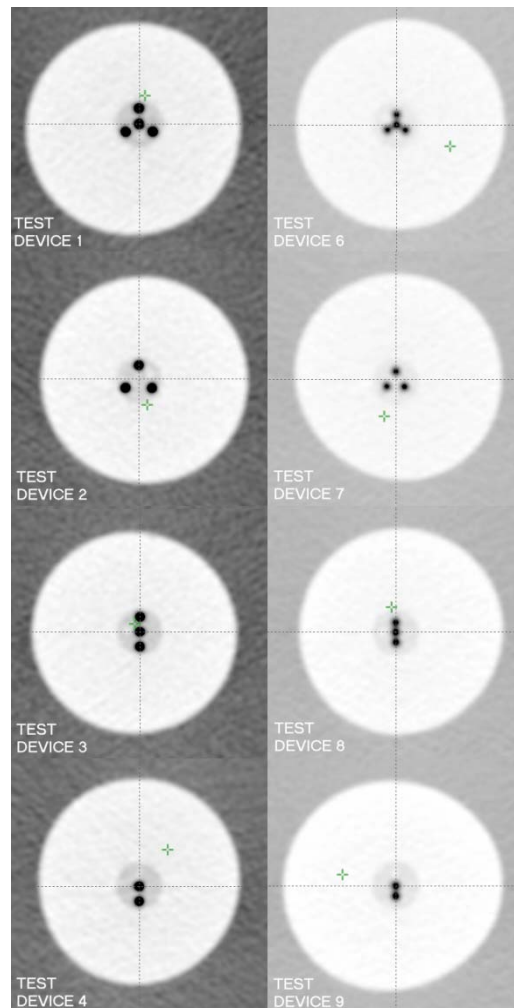


Fig. 1 – Cross – sections of test devices.

## 2.2. IMAGING

The balloons were inflated using a mixture of 5 vol.% contrast solution in 0.9% saline water. The contrast was used to obtain a better visual differentiation of the balloon in a homogeneous media (water is our case). At least two diameters of the inflated balloons were checked using a caliper, and the balloon diameter found is 40 mm. Caution was exercised at the time of inflation, in order to avoid formation of air bubbles inside the balloons.

An experimental device was created in which the balloons were suspended in water for simulate the actual clinical conditions.

A small positioning device was placed on the bottom of the water bath and taped on the positioning device at about 4 cm from the bottom and the alignment was checked. The water level was verified at all times and found to be at least 4 cm above the balloons. A thin plastic plate was placed on top of the water in order to minimize water waves during scanning.

The experimental device was aligned on the CT table using the internal and wall mounted lasers. We acquired anterior-posterior and lateral scouts. Each test device was imaged using a helical scanning technique with 2.5 mm slice width. The Field of View (FOV) was adjusted in order to obtain the optimal coverage of the balloon while maintaining a minimum of 4 cm distance above and below the device. An average of 60 slices was obtained for each CT study. The images quality and artifacts were evaluated. The symmetry, distance between the lumens as well as the distance from the balloon surface to the edges of the water phantom were determined.

### 2.3. TREATMENT PLANNING

The CT images were exported to the BrachyVision Planning Station (Varian Medical Systems, Inc, Varian Oncology Systems, Charlottesville, VA). Each test device was evaluated in axial and multiplanar reconstruction views for skin spacing, symmetry and conformance of the applicator. The structures created simulate all potential clinical conditions.

The Body structure was reconstructed by the BrachyVision software following the import of CT studies into the system. Several structures associated with the device and with the hypothetical surrounding healthy tissue were created. The Body represents the body contour when the distance between the balloon surface and the skin surface is larger than 10 mm. Body 1 represents the body contour when the distance between the balloon surface and the skin surface is larger than 5 mm with no more than 3 consecutive CT slices less than 5 mm and 1 lumen is oriented towards the skin. Following the same pattern, Body 2 represents the body contour when the distance between the balloon surface and the skin surface is larger than 5 mm with no more than 3 consecutive CT slices less than 5 mm and 2 lumens are oriented toward the skin.

*MammoSite* (MS) represents the actual reconstructed balloon of the test device. MS+1+Opt represents the actual balloon plus 1 cm margin in all directions when the distance between the balloon surface and the skin surface is larger than 10 mm (Body) and it is used to generate other structures and for volume optimization at its surface. In the same scheme MS+1+Opt1 and MS+1+Opt2 represent the actual balloon plus 1 cm margin in all directions and 1 lumen is oriented toward the skin (Body 1), respectively 2 lumens are oriented towards the skin (Body 2).

The *Planning Target Volume* (PTV) was generated as a uniform layer of 1 cm around the MS structure when the distance between the balloon surface and the skin surface is larger than 10 mm (Body). Subsequently PTV1 and PTV2 were created as a uniform layers of 1 cm around the MS structure except when the distance from the balloon to the skin was 5 mm over a continuous length of 1 cm at the surface of the skin.

Healthy Breast, Hath Breast 1 and 2 tissues were created as a 2 cm layer around the PTV. in direct correlation to the definition of Body, Body 1 and Body 2. The structures created for optimization purposes are presented in Fig. 2.

The prescribed dose was 340 cGy per fraction to the surface of PTV, PTV1 and PTV2. The planning criteria applied in these cases followed the National Surgical Adjuvant Breast and Bowel Project B-39/Radiation Therapy Oncology Group 0413 [29] guidelines for APBI irradiation with respect to D90, V100, V150, V200 and MSD. D90 represents the percentage of the prescribed dose delivered to 90% of the PTV, MSD is the Maximum Skin Dose, while V150 and V200 represent the volumes covered by the dose (in %). Wazer *et al.* [30] first showed that escalated values for these entities are linked to the development of fat tissue necrosis. Lately, several authors [25-27] analyzed tolerances and toxicities related to these dosimetric parameters.

The Coverage Index (CI) is a measure of the fraction of the breast target volume receiving a dose equal to, or greater than the prescribed dose. The External Index (EI) was calculated by dividing the volume of Healthy Breast that is receiving at least 340 cGy/fraction by the total volume of the whole breast volume.

The planning criteria are presented in Table 2. The number of lumens, radiation source positions used and size of dwell times were chosen in such a manner as to deliver an optimal dose coverage of the target volume based on the optimization goals displayed in Table 2.

Each device has an arbitrary position in the tissue and the minimum skin and chest wall spacing is equal or greater than 10 mm. Then, two additional scenarios were considered. One catheter (a) and two catheters (b) are oriented toward the skin, with a minimum skin spacing of 5 mm for 1 cm<sup>2</sup> and a minimum chest wall spacing equal or greater than 10 mm.

Depending on the device's design, two or three sets of plans were created for each of the scenarios described above. A total of 52 dosimetry treatment plans were developed. The isodose distributions for all the plans were obtained by volume optimization of the MS+1cm+Opt structures, followed by slight manual adjustments. All the plans generated for each of the situations described above were evaluated by means of dose volume histogram (DVH) analysis.

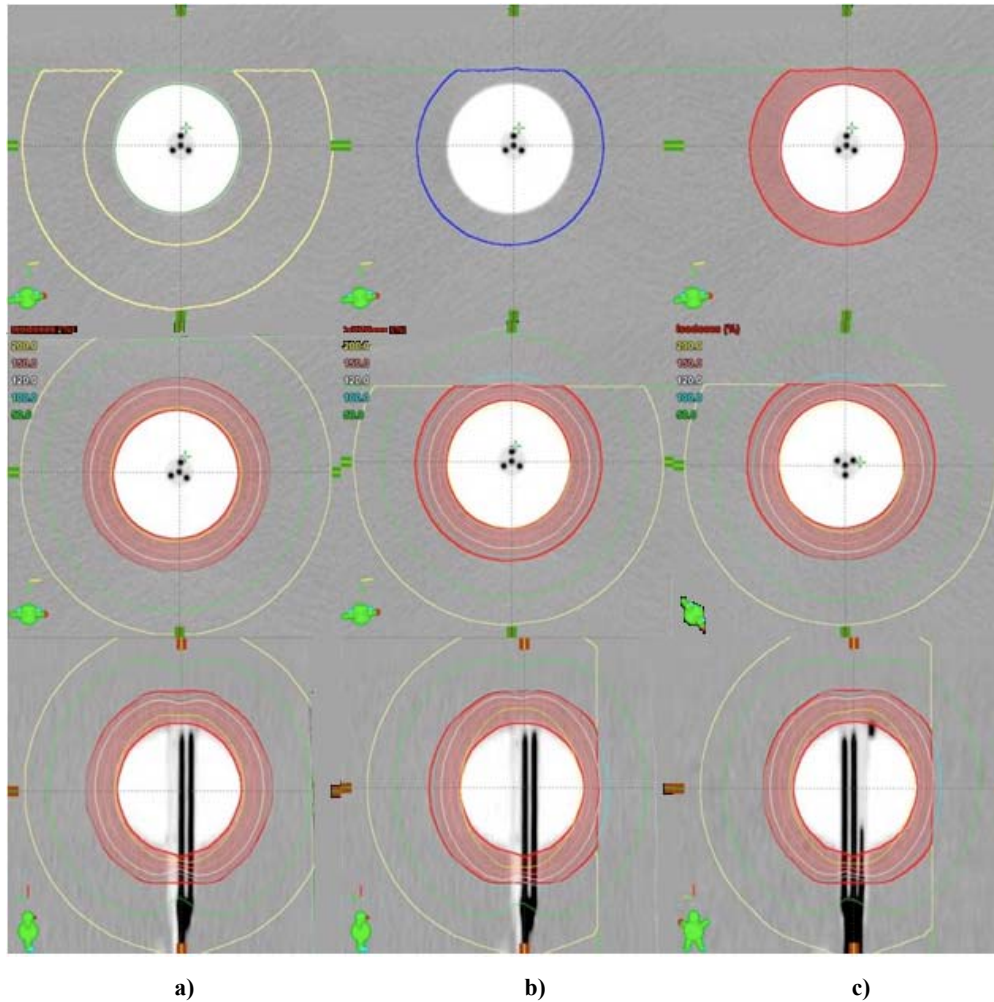


Fig. 2 – Structures created for optimization purposes: a) represents the Healthy Breast structure; b) represents the MS+1+Opt structure and c) represents the PTV.

Table 2

Planning criteria

Planning Criteria	D90	V150	V200	MSD	CI	EI
1	>90%	$\leq 50(\text{cm}^3)$	$\leq 10(\text{cm}^3)$	$\leq 145\%$	High	$\leq 5\%$
2	>90%	$\leq 50(\text{cm}^3)$	$\leq 10(\text{cm}^3)$	$\leq 120\%$	$\geq 90\%$	$\leq 5\%$
3	=90%	$\leq 50(\text{cm}^3)$	$\leq 10(\text{cm}^3)$	Low	-	$\leq 5\%$

### 3. RESULTS AND DISCUSSIONS

For all devices and clinical situations, above described, the PTV volumes were found to have a mean value of 81.95 (cm<sup>3</sup>) and standard deviation of  $\pm 2.06$ .

One set of plans was optimized for high *Coverage Index* (CI) and high D90, with a Max Skin Dose less than 145% (493 cGy), EI  $\leq 5\%$ , V150  $\leq 50$  (cm<sup>3</sup>) and V200  $\leq 10$  (cm<sup>3</sup>). Relevant details are listed in Table 3.

For all clinical situations the MSD was kept under 493 cGy with a maximum value of 475.1 cGy for the test device #5, planned with 1 catheter towards the skin. The CI was well above 90% with a minimum of 95.2% for the test device #5. For all the clinical situations the EI was below 2% with a maximum of 1.586% for the test device #3 and the plan developed with 1 catheter toward the skin. More than 100% of prescription dose delivered to 90% of the PTV was obtained for all three clinical situations. As we expected, V150 and V200 were kept below 50 cm<sup>3</sup> respectively 10 cm<sup>3</sup>, for all dosimetric plans created for these dose constraints.

The second set of plans was developed having less than 120% (408 cGy) MSD and high D90, CI  $\geq 90\%$ , EI  $\leq 5\%$ , V150  $\leq 50$  (cm<sup>3</sup>) and V200  $\leq 10$  (cm<sup>3</sup>) as main optimization goals.

In this case was possible to keep the MSD below 120% from the prescription dose and still achieve an optimal CI as well as a high D90. The MSD of 408 cGy and the lowest CI of 90.7% were obtained for test device #1 in the scenario with one catheter toward the skin. In all situations EI, V150, V200 were well below 5%, 50 cm<sup>3</sup> and 10 cm<sup>3</sup> respectively. D90 was more than 100% for all the devices and clinical situations considered for the present study.

For the first two categories the results are in good agreement with those published previously for single-lumen MammoSite [13–16], but as we expected to be better than those obtained with interstitial brachytherapy [31].

A third set of plans was also created to demonstrate that even in the most challenging clinical situations (*i.e.* distance to skin of 5 mm in more than 3 slices, which with the simple MS device was considered an exclusion criteria [29]) we can still achieve a low skin dose while maintaining the criteria described in Table 2.

Table 3

Results of plan optimization for high CI, high D90 & Max Skin Dose < 145% when the minimum skin spacing is 5 mm

Device #	Device position	MSD (cGy)	CI (%)	EI (%)	D90 (%)	V150 (cm <sup>3</sup> )	V200 (cm <sup>3</sup> )
1	1 cts <sup>a</sup>	455.1	98.4	0.493	106.0	31.0	8.6
1	2 cts	466.0	98.4	0.695	106.5	31.5	8.9
2	1 cts	455.9	99.0	0.592	106.5	31.0	8.9
2	2 cts	464.7	99.0	1.092	107.8	32.1	9.6
3	1 cts	455.8	95.7	1.586	106.1	31.5	9.6

Table 3 (continued)

4	1 cas <sup>b</sup>	430.1	97.6	1.218	107.3	31.3	8.7
5	1 cts	475.1	95.2	0.764	104.6	2.5	8.3
6	1 cts	456.6	98.4	0.558	106.1	31.0	8.4
6	2 cts	469	98.4	0.468	105.9	31.0	8.4
7	1 cts	449.1	97.5	0.335	104.9	29.9	7.6
7	2 cts	451.1	97.5	0.868	106.3	31.2	8.6
8	1 cts	449.4	97.5	1.170	107.1	31.2	8.5
9	1 cas	472.4	96.5	0.942	105.8	31.2	8.5
10	1 cts	449.6	96.5	0.372	104.4	30.0	6.9

<sup>a</sup>cts – catheter toward skin

<sup>b</sup>cas – catheter away from skin

For the situation when the devices have an arbitrary position in the phantom (tissue) and the minimum skin and chest wall spacing is at least 10 mm all the optimization goals described in Table 2 are successfully met by all the balloons studied. As expected, the MSD was kept below 100% of the prescription dose. The CI was above 95% for all situations with a minimum of 95.2 % and a max of 99% having a mean value of 97.54% and standard deviation of 1.18. The EI was kept well below 2% for all devices with a minimum of 0.263% and a max of 1.586%. D90 was above 104% for all the cases. V150 was found to be below 50cc with a maximum value of 32.1 cc and V200 was kept below 10cc without any difficulty.

The asymmetry of these devices was determined by measuring opposing radii and dividing their difference by 2. The asymmetry of all 10 test devices was found to be acceptable (less than 2 mm). An advantage of the multi-lumen test devices over the MS is that they can compensate in most of the situations for the asymmetry of the balloon. If the treatment plan meets all the reference criteria (CI, D90, MSD, V150, V200, and EI) the asymmetry should not be an issue.

As all test devices were able to achieve the goals of this study, it is difficult to dosimetrically rank them, especially since their asymmetry is different. However, after taking into account all the planning aspects, the flexibility and complexity of the dose optimization for any clinical situation, we can state that test device #1 (Fig. 1) has the best configuration. Its configuration with 3 mm offset of the lumen center to balloon shaft center can achieve a more off-center dose coverage in practice. Another notable attribute of test device #1 is the fact that it can achieve a dose shift in multiple planes, compared to the other devices tested which can achieve a dose shift only in one plane (test device #3) or none at all.

This work brings further proof that a multilumen design provides more flexibility in patient selection, planning and dosimetric outcome. The possibility of planning with all or just a few of the lumens offers a better control of the dose distribution with significantly lower dose at the skin, chest wall and lung level as previously reported [25–27].

Furthermore, we proved that even in the most challenging clinical situations the dose to the skin can be kept at 100% of the prescription dose while maintaining most of the other dosimetric parameters in their optimal range.

#### 4. CONCLUSION

In this dosimetrical study all the reference criteria were easily achieved by each of the ten devices for all clinical situations investigated. Each of the test devices can drastically reduce the skin dose comparative to any symmetrical MS of the same balloon size while meeting all the reference criteria. This was not achievable for any symmetrical MS.

Although all 10 MSML test devices are dosimetrically superior to the symmetrical MS of the same balloon size, the prototype device #1 may have the optimum configuration for a MSML to be used in APBI.

*Acknowledgements.* We thank Dr. Jeff Dorton (Hologic, Inc.) for helpful guidance and constructive feedback.

#### REFERENCES

1. B. Fisher, S. Anderson, C.K. Redmond, N. Wolmark, L. Wickerham, W.M. Cronin, *N. Engl. J. Med.*, **333**, 1456 (1995).
2. F. Vicini, V.R. Kini, P.Y. Chen, E. Horwitz, G. Gustafson, P. Benitez, G. Edmundson, N. Goldstein, K. McCarthy, A. Martinez, *J. Surg Oncol.*, **70**, 33 (1999).
3. K.L. Baglan, A.A. Martinez, R.C. Frazier, V.R. Kini, L.L. Kestin, P.Y. Chen, G. Edmundson, E. Mele, D. Jaffray, F.A. Vicini, *Int. J. Radiat. Oncol. Biol. Phys.*, **50**, 1003 (2001).
4. F.A. Vicini, P.Y. Chen, M. Fraile, G.S. Gustafson, G.K. Edmundson, D.A. Jaffray, P. Benitez, J. Pettinga, B. Madrazo, J.A. Ingold, N.S. Goldstein, R.C. Matter, A.A. Martinez, *Int. J. Radiat. Oncol. Biol. Phys.*, **38**, 301 (1997).
5. F.A. Vicini, L.L. Kestin, G.K. Edmundson, D.A. Jaffray, J.W. Wong, V.R. Kini, P.Y. Chen, A.A. Martinez, *Int. J. Radiat. Oncol. Biol. Phys.*, **45**, 803 (1999).
6. L.L. Kestin, D.A. Jaffray, G.K. Edmundson, A.A. Martinez, J.W. Wong, V.R. Kini, P.Y. Chen, F.A. Vicini, *Int. J. Radiat. Oncol. Biol. Phys.*, **46**, 35 (2000).
7. I.S. Fentiman, C. Poole, D. Tong, P.J. Winter, W.M. Gregory, H.M.O. Mayles, P. Turner, M.A. Chaudary, R.D. Rubens, *Eur. J. Cancer*, **32A**, 608 (1996).
8. P.R. Benitez, P.Y. Chen, F.A. Vicini, M. Wallace, L. Kestin, G. Edmundson, G. Gustafson, A. Martinez, *Am. J. Surg.*, **188**, 355 (2004).
9. K.L. Baglan, M.B. Sharpe, D. Jaffray, R.C. Frazier, J. Fayad, L.L. Kestin, V. Remouchamps, A.A. Martinez, J. Wong, F.A. Vicini, *Int. J. Radiat. Oncol. Biol. Phys.*, **55**, 302 (2003).
10. F.A. Vicini, V. Remouchamps, M. Wallace, M. Sharpe, J. Fayad, L. Tyburski, N. Letts, L. Kestin, G. Edmundson, J. Pettinga, N.S. Goldstein, J. Wong, *Int. J. Radiat. Oncol. Biol. Phys.*, **57**, 1247 (2003).
11. M. Intra, G. Gatti, A. Luini, V. Galimberti, P. Veronesi, S. Zurrida, A. Frasson, M. Ciocca, R. Orecchia, U. Veronesi, *Arch. Surg.*, **137**, 737 (2002).

12. J.S. Vaidya, J.S. Tobias, M. Baum, M. Keshtgar, D. Joseph, F. Wenz, J. Houghton, C. Saunders, T. Corica, D. D'Souza, R. Sainsbury, S. Massarut, I. Taylor, B. Hilaris, *Lancet Oncol.*, **5**, 165 (2004).
13. G.K. Edmundson, F.A. Vicini, P.Y. Chen, C. Mitchell, A.A. Martinez, *Int. J. Radiat. Oncol. Biol. Phys.*, **52**, 1132 (2002).
14. M. Keisch, F. Vicini, R.R. Kuske, M. Hebert, J. White, C. Quiet, D. Arthur, T. Scroggins, O. Streeter, *Int. J. Radiat. Oncol. Biol. Phys.*, **55**, 289 (2003).
15. A. Dickler, M. Kirk, J. Choo, W.C. Hsi, J. Chu, K. Dowlatshahi, D. Francescatti, C. Nguyen, *Int. J. Radiat. Oncol. Biol. Phys.*, **59**, 469 (2004).
16. K.K. Chao, F.A. Vicini, M. Wallace, C. Mitchell, P. Chen, M. Ghilezan, S. Gilbert, J. Kunzman, P. Benitez, A. Martinez, *Int. J. Radiat. Oncol. Biol. Phys.*, **69**, 32 (2007).
17. L.W. Cuttino, D.W. Arthur, M. Keisch, J.M. Jenrette, B.R. Prestidge, C.A. Quiet, F.A. Vicini, J. Rescigno, D.E. Wazer, R. Patel, *Int. J. Radiat. Oncol. Biol. Phys.*, **66**, S30 (2006).
18. J.L. Harper, J.M. Jenrette, K.N. Vanek, E.G. Aguero, W.E. Gillanders, *Int. J. Radiat. Oncol. Biol. Phys.*, **61**, 169 (2005).
19. P.R. Benitez, M.E. Keisch, F. Vicini, A. Stolier, T. Scroggins, A. Walker, J. White, P. Hedberg, M. Hebert, D. Arthur, V. Zannis, C. Quiet, O. Streeter, M. Silverstein, *Am. J. Surg.*, **194**, 456 (2007).
20. B. Prestidge, A. Sadeghi, A. Rosenthal, L. Salinas, S. Zubyk, *Int. J. Radiat. Oncol. Biol. Phys.*, **66**, S215 (2006).
21. C. Yashar, D. Scanderbeg, R. Kuske, A. Wallace, V. Zannis, S. Blair, E. Grade, V.H. Swenson, C. Quiet, *Int. J. Radiat. Oncol. Biol. Phys.*, 2010; DOI: 10.1016/j.ijrobp.2010.018.
22. C. Cross, A. Brown, P. Escobar, W. Kokal, C. Mantz, *Int. J. Radiat. Oncol. Biol. Phys.*, **72**, S182 (2008).
23. S. Gurdalli, R. Kuske, C.A. Quiet, V. Howard, *Brachytherapy*, **7**, 142 (2008).
24. D. J. Scanderbeg, C. Yashar, R. Rice, T. Pawlicki, *Radiother. Oncol.*, **90**, 36 (2009).
25. L.W. Cuttino, D. Todor, M. Rosu, D.W. Arthur, *Brachytherapy*, **8**, 223 (2009).
26. D.W. Arthur, F.A. Vicini, D.A. Todor, T.B. Julian, M.R. Lyden, *Int. J. Radiat. Oncol. Biol. Phys.*, **79**, 26 (2011).
27. S. Brown, M. McLaughlin, K. Pope, K. Haile, L. Hughes, P.Z. Israel, *Brachytherapy*, **8**, 227 (2009).
28. R.B. Wilder, L.D. Curcio, R.K. Khanijou, M.E. Eisner, J.L. Kakkis, L. Chittenden, J. Agustin, J. Lizarde, A.V. Mesa, J. Ravera, K.M. Tokita, *Brachytherapy*, **8**, 373 (2009).
29. NSABP Protocol B-39, RTOG Protocol 0413.
30. D.E. Wazer, D. Lowther, T. Boyle, K. Ulin, A. Neuschatz, R. Ruthazer, T.A. DiPetrillo, *Int. J. Radiat. Oncol. Biol. Phys.*, **50**, 107 (2001).
31. D.E. Wazer, S. Kaufman, L. Cuttino, T. DiPetrillo, D.W. Arthur, *Int. J. Radiat. Oncol. Biol. Phys.*, **64**, 489 (2006).